2009

Global voltage unbalance in MV networks due to line asymmetries

Prabodha Paranavithana
University of Wollongong, ptp123@uow.edu.au

Sarath Perera
University of Wollongong, sarath@uow.edu.au

Robert Koch
Eskom Holdings Limited Sth Africa

Z. Emin
National Grid Electricity Transmission, U.K.

Publication Details

P. Paranavithana, S. Perera, R. Koch & Z. Emin, "Global voltage unbalance in MV networks due to line asymmetries," IEEE Transactions on Power Delivery, vol. 24, (4) pp. 2353-2360, 2009.

Global Voltage Unbalance in MV Networks Due to Line Asymmetries

P. Paranavithana, *Student Member, IEEE*, S. Perera, *Member, IEEE*, R. Koch, and Z. Emin

***Abstract*—The International Electrotechnical Commission (IEC) has recently released the Technical Report IEC/TR 61000-3-13 for the assessment of voltage unbalance emission limits to individual customer installations connected to medium-voltage (MV), high-voltage, and extra–high-voltage power systems. As in the counterpart IEC technical reports for harmonics (IEC 61000-3-6) and flicker (IEC 61000-3-7) allocation, IEC/TR 61000-3-13 also apportions the global emission allowance to customers in proportion to their agreed apparent power. However, noting that voltage unbalance at a busbar can arise due to load and system (essentially lines) asymmetries, IEC/TR 61000-3-13 applies a scaling factor Kue to the apportioned allowance. Tis factor Kue represents the fraction of the global emission allowance that can be allocated to installations. Conversely, the factor $K'ue = 1 - Kue$ accounts for the emission arising as a result of system inherent asymmetries. This paper addresses the global voltage unbalance emission in MV power systems arising as a result of line asymmetries on which a systematic evaluation method is not given in IEC/TR 61000-3-13. First, a detailed study with the view to investigate the influence of line asymmetries on the global emission and its dependency on various load types is carried out by employing a simple radial network. Second, a matrix-based methodology, covering radial and interconnected networks, for the assessment of this emission at the nodal level taking line, system and load characteristics, system operating conditions, and downstream load composition into account are proposed. The methodology is verified by using unbalance load-flow analysis.**

***Index Terms*—Line asymmetries, medium-voltage (MV) power systems, radial and interconnected networks, voltage unbalance, voltage unbalance allocation.**

I. Introduction

CIGRE/CIRED Joint Working Group C4.103 has been active in developing guidelines for determining negative-sequence voltage unbalance emission limits to three-phase unbalanced installations connected at different voltage levels of power systems [1]–[3]. As an outcome, the new Technical Report IEC/TR 61000-3-13 [4] has been recently released which enables system operators to coordinate voltage unbalance between various voltage levels so that adequate service quality to connected customers is ensured.

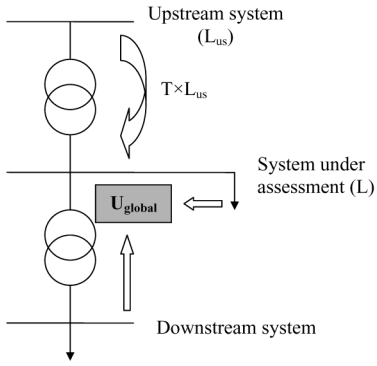

Fig. 1. Illustration of the voltage unbalance coordination principle used in IEC/TR 61000-3-13 [4].

The philosophy of IEC/TR 61000-3-13 is similar to that of the counterpart IEC recommendations for harmonics (IEC 61000-3-6 [5]) and flicker (IEC 61000-3-7 [6]) allocation. Compatibility levels are used as reference values for coordinating the emission and the immunity of equipment or installations which are part of, or supplied by, a power system in order to ensure the electromagnetic compatibility (EMC) in the whole system. The coordination of voltage unbalance between various voltage levels is achieved by means of planning levels (set as internal quality objectives) so that compatibility levels are not exceeded. The general principle used to coordinate the disturbance is such that the total emission level derived by using the general summation law, taking the upstream contribution in terms of a transfer coefficient into account, at any point, should not exceed the set planning level. An illustration of this principle is given by using a simple radial system in Fig. 1. Based on this principle, the system absorption capacity or the global emission allowance is established as [4]

$$U_{\text{global}} = \sqrt[\alpha]{(L)^{\alpha} - (TL^{us})^{\alpha}} \tag{1}$$

where

- L, L^{us} planning levels of the system under assessment and the upstream (US) system, respectively;
- α summation law exponent;
- T transfer coefficient from the upstream system to the downstream system under assessment;
- U_{global} global emission (i.e., from the unbalanced installations and line asymmetries existing in the system under assessment and its downstream lower voltage systems) allowance.

Manuscript received December 03, 2008; revised February 18, 2009. Current version published September 23, 2009. Paper no. TPWRD-00777-2008.

P. Paranavithana and S. Perera are with the School of Electrical, Computer and Telecommunications Engineering, University of Wollongong. They are also with the Integral Energy Power Quality and Reliability Centre, Wollongong NSW 2522, Australia (e-mail: sarath@uow.edu.au).

R. Koch is with the Eskom Holdings Limited, Resources and Strategy Division, Eskom Research and Innovation Centre, Cleveland 2022, South Africa.

Z. Emin is with the National Grid Electricity Transmission, Asset Management, System Technical Performance, Warwick Technology Park, Gallows Hill, Warwick CV34 6DA, U.K.

Color versions of one or more of the figures in this paper are available online at http://ieeexplore.ieee.org.

Digital Object Identifier 10.1109/TPWRD.2009.2028503

Global emission allowance U_{global} is apportioned to various busbars (say, U^x_{global} for a busbar x) of the considered system in proportion to the ratio between the total apparent power supplied by the busbar and the total apparent power supplied by the entire system as seen at the busbar. In relation to harmonics and flicker, this total busbar allowance U^x_{global} is then allocated to individual customers which are to be connected at the busbar in proportion to the ratio between the agreed apparent power and the total apparent power supplied by the busbar. However, in the case of voltage unbalance, the allocation of the total U^x_{global} to installations can result in excessive voltage unbalance levels noting that the global emission at a busbar generally arises not only from unbalanced installations (U^x_{loads}) but also from system inherent asymmetries (U^x_{lines}). That is

$$\left(U^x_{\text{global}}\right)^{\alpha} = (U^x_{\text{loads}})^{\alpha} + (U^x_{\text{lines}})^{\alpha}. \tag{2}$$

This issue has been addressed in IEC/TR 61000-3-13 by introducing a new factor Kue, which is defined by (3). This Kue represents the fraction of U^x_{global} that can be allocated to unbalanced installations. Conversely, the factor $K'ue = 1 - Kue$, which is given by (4), represents the fraction of U^x_{global} that accounts for the emission arising from system inherent asymmetries

$$Kue^x = \left(\frac{U^x_{\text{loads}}}{U^x_{\text{global}}}\right)^{\alpha} \tag{3}$$

$$K'ue^x = \left(\frac{U^x_{\text{lines}}}{U^x_{\text{global}}}\right)^{\alpha}. \tag{4}$$

The busbar emission allowance U^x_{global} is then allocated to individual installations which are to be connected at the busbar as [4]

$$E^x_j = \sqrt[\alpha]{Kue^x}\, U^x_{\text{global}} \sqrt[\alpha]{\frac{S^x_j}{S^x_{\text{total}}}} \tag{5}$$

where,

E^x_j emission limit to an installation j which is to be connected at the busbar x;

S^x_j agreed apparent power of the installation j;

S^x_{total} total apparent power to be supplied by the busbar x.

IEC/TR 61000-3-13 recommends system operators to assess the factor $K'ue$ for prevailing line construction practices and system characteristics in their specific networks. However, a systematic method for its evaluation is not provided other than a rudimentary direction together with a set of indicative values. Referring to the specifics of the direction mentioned before, the global voltage unbalance U^{rec}_t (in terms of the voltage unbalance factor) caused by a radial asymmetrical line (overhead, single circuit) at its receiving end busbar can be derived by using[1][4]

$$U^{\text{rec}}_t \approx \frac{|Z_{-+:t} I_{+:t}|}{V_{n-p}} \tag{6}$$

[1]Nominal system voltage is taken as the prevailing positive-sequence voltage at the busbar.

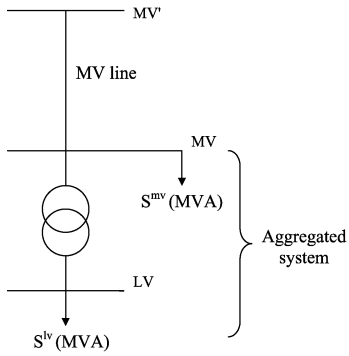

Fig. 2. MV–LV radial system.

where

t asymmetrical line;

$Z_{-+:t}$ coupling impedance between negative- and positive-sequence networks of the line t;

$I_{+:t}$ positive-sequence current in the line t;

V_{n-p} nominal phase voltage of the system.

It has been seen that (6) is acceptable in the presence of passive loads (e.g., constant power) [7]. However, its validity is questionable especially for an untransposed MV line supplying an industrial load base containing a large proportion of three-phase induction motors due to relatively high levels of negative-sequence currents drawn by induction motors in the presence of voltage unbalance. A set of indicative values given for $K'ue$ in IEC/TR 61000-3-13 also intimates that $K'ue$ is related to the proportion of induction motors. These emphasize that although by the definition $K'ue$ is a parameter which accounts for system inherent asymmetries, it has some degree of load dependency which is an aspect that requires detailed examinations.

Objectives of the work presented in this paper are to:

- investigate the influence of line asymmetries on the global voltage unbalance in MV power systems and its dependency on various load types/bases; related work carried out by using a simple radial system is presented in Section II;
- develop a generalized methodology, covering radial and interconnected networks, for evaluating this global emission; this is given in Section III.

The results that have been established by using the proposed methodology have been compared against the results obtained from the unbalanced load-flow analysis [9] in Section IV. Conclusions are given in Section V.

II. Influence of Line Asymmetries on the Global Emission and its Dependency on Loads

Consider the MV–LV radial system shown in Fig. 2 where the MV line (t) of interest is untransposed. The purpose is to assess the voltage unbalance (U^{mv}_t) caused by the line at its receiving-end busbar (i.e., a busbar labelled as MV) while the voltages at the sending-end busbar MV' are balanced. For this, the loads S^{mv} and S^{lv} are considered to be balanced.

Voltage unbalance U_t^{mv} can be generally expressed[2] as

$$U_t^{\mathrm{mv}} = \left| \frac{V_-^{\mathrm{mv/t}}}{V_+^{\mathrm{mv}}} \right| \tag{7}$$

where

$$|V_-^{\mathrm{mv/t}}| = |Z_{-+:t} I_{+:t} + Z_{--:t} I_{-:t/t}| \tag{8}$$

$V_-^{\mathrm{mv/t}}$ negative-sequence voltage at the busbar MV caused by the line t;

V_+^{mv} positive-sequence voltage at the busbar MV;

$Z_{--:t}$ negative-sequence impedance of the line$t$, which is inherently equal to its positive-sequence impedance $Z_{++:t}$;

$I_{-:t/t}$ negative-sequence current in the line t arising as a result of the line t itself.

The work presented in [8] suggests that the impact of the term $Z_{++:t} I_{-:t/t}$ or the negative-sequence current $I_{-:t/t}$ on the resulting voltage $|V_-^{\mathrm{mv/t}}|$ depends on the load type/base supplied by the system making the voltage unbalance U_t^{mv} dependent on the load type. The purpose of this section is to examine the influence of four basic load types (constant impedance, constant current, constant power, and three-phase induction motor loads) on the voltage unbalance U_t^{mv}.

1) Constant Impedance (Z) Loads: When S^{mv} and S^{lv} (Fig. 2) represent constant impedance loads (balanced—decoupled and equal positive: $Z_{++:z_l}$, negative: $Z_{--:z_l}$ and zero-sequence impedances), (8) can be simplified by using the decoupled nature of sequence impedances of the loads as (Appendix A)

$$|V_-^{\mathrm{mv/t}}| = |Z_{-+:t} I_{+:t}| \left| \frac{Z_{--}^{\mathrm{mv}}}{Z_{--}^{\mathrm{mv'}}} \right| \tag{9}$$

where Z_{--}^{mv}, $Z_{--}^{\mathrm{mv'}}$ are the downstream negative-sequence impedances seen at the busbars MV and MV', respectively. Equation (9) can be rearranged by using $Z_{++:z_l} = Z_{--:z_l}$ as

$$|V_-^{\mathrm{mv/t}}| \approx |Z_{-+:t} I_{+:t}| \ (1 - VR_t) \tag{10}$$

where $VR_t = \left| \frac{Z_{++:t} I_{+:t}}{V_+^{\mathrm{mv'}}} \right|$ is the voltage regulation of the line t and $V_+^{\mathrm{mv'}}$ is the positive-sequence voltage at the busbar $\mathrm{MV'}$.

That is, for constant impedance loads, the negative-sequence current $I_{-:t/t}$ impacts in such a manner that the term $Z_{++:t} I_{-:t/t}$ causes the voltage $|V_-^{\mathrm{mv/t}}|$ to be smaller than that predicted by using $|Z_{-+:t} I_{+:t}|$ considered in (6)[3] by the factor $(1 - VR_t)$.

2) Constant Current (I) Loads: Negative-sequence current $I_{-:t/t}$ in (8) can be considered to be negligible when the system supplies constant current loads (balanced), since these loads draw equal magnitudes of three-phase currents regardless of the prevailing voltage condition. Hence, (8) can be simplified for these loads as

$$|V_-^{\mathrm{mv/t}}| \approx |Z_{-+:t} I_{+:t}|. \tag{11}$$

That is, in contrary to the case of constant impedance loads, the direction given in IEC/TR 61000-3-13 by (6) requires no modifications for constant current loads. The difference between the behaviors exhibited by constant current loads and constant impedance loads is essentially due to the way how these loads react when the supply voltage is unbalanced. In the former case, the currents will be nearly balanced, giving rise to no negative-sequence current, whereas in the latter case, there will be a flow of negative-sequence current although the impedances are balanced.

3) Constant Power (PQ) Loads: Since linearization of system equations and simplifying assumptions (as in the case of constant current loads) is not supported by constant power loads, results obtained from unbalanced load-flow analysis were analyzed and (12) is established for operating scenarios that are most likely to occur in practice as a closer approximation to $|V_-^{\mathrm{mv/t}}|$

$$|V_-^{\mathrm{mv/t}}| \approx |Z_{-+:t} I_{+:t}| \ (1 - VR_t)^{\beta} \tag{12}$$

where $\beta \approx -1$ and -2 for low (~ 0.9) and high (~ 1) lagging power factor (lag. pf) loading conditions, respectively[4]. That is, for constant power loads, the negative-sequence current $I_{-:t/t}$ behaves such that the term $Z_{++:t} I_{-:t/t}$ causes the voltage $|V_-^{\mathrm{mv/t}}|$ to be higher than the term $|Z_{-+:t} I_{+:t}|$ considered in (6) by the factor $(1 - VR_t)^{\beta}$.

Taking a generalized view, the additional factors associated with the aforementoned proposed expressions: (10)–(12) with respect to the direction given in IEC/TR 61000-3-13 by (6) can be expressed in a form $(1 - VR_t)^{\gamma}$ for the three basic passive load types (where $\gamma = 1$ for constant impedance loads, $\gamma = 0$ for constant current loads, and $-2 \leq \gamma \leq -1$ for constant power loads). Considering most practical circumstances where VR_t <10%, the factor $(1 - VR_t)^{\gamma}$ can be approximated to a value of unity (in other words, $I_{-:t/t} \approx 0$). That is, for passive loads, the negative-sequence voltage $|V_-^{\mathrm{mv/t}}|$ can be approximately established by using the term $|Z_{-+:t} I_{+:t}|$ as indicated in IEC/TR 61000-3-13.

4) Induction Motor (IM) Loads: Three-phase induction motors (supplied at LV (i.e., $S^{\mathrm{mv}} = 0$) can be represented by using decoupled, unequal, and constant (for a given motor speed) sequence impedances. Hence, (8) can be simplified to the form given by (9) which can be re-expressed for induction motor loads as[5]

$$|V_-^{\mathrm{mv/t}}| \approx |Z_{-+:t} I_{+:t}| \frac{1}{1 + \left(\frac{VR_t}{1 - VR_t} \right) \left(\frac{1}{\frac{1}{k_s} + \frac{1}{k_{sc}^{\mathrm{lv}}}} \right)} \tag{13}$$

[2]The impact of zero-sequence variables is ignored since IEC/TR 61000-3-13 considers that they can be controlled through system design and maintenance.

[3]This neglects the impact of the term $Z_{++:t} I_{-:t/t}$ on the resulting voltage $|V_-^{\mathrm{mv/t}}|$.

[4]β depends only on the load power factor.

[5]This specific case with $k_{sc}^{\mathrm{lv}} = 1$ and $k_m = 1$ can be deduced by using the generalized expression (18) of which the derivation is given in Appendix C.

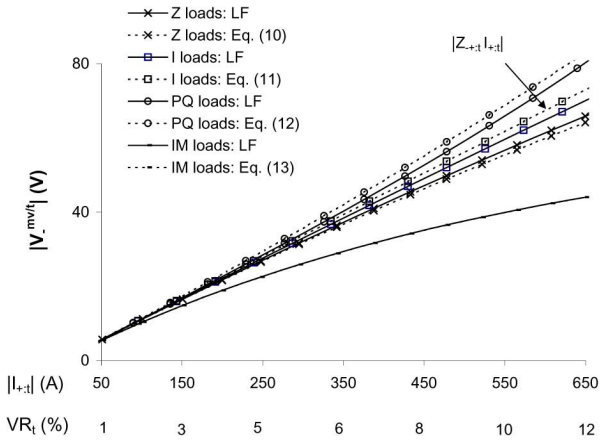

Fig. 3. Variation of $|V_-^{\mathrm{mv/t}}|$ with $|I_{+:t}|$ (VR_t values corresponding to various $|I_{+:t}|$ are also indicated) for the four basic load types.

where

k_s ratio between the positive-sequence and the negative-sequence impedances of the aggregated motor load supplied by the LV system (typically, $5 < k_s < 7$)

$$k_{sc}^{\mathrm{lv}} = \frac{\mathrm{SCC}^{\mathrm{lv}}}{S^{\mathrm{lv}}}$$

$$\mathrm{SCC}^{\mathrm{lv}} = \frac{(V_n^{\mathrm{lv}})^2}{|Z_{++:\mathrm{ml-lv}}|}$$

V_n^{lv} nominal line-to-line voltage of the LV system;

$Z_{++:\mathrm{ml-lv}}$ positive-sequence impedance of the aggregated MV–LV transformer referred to LV.

That is, the negative-sequence current $I_{-:t/t}$ behaves so that the term $Z_{++:t}I_{-:t/t}$ causes the voltage $|V_-^{\mathrm{mv/t}}|$ to be smaller than the term $|Z_{-+:t}I_{+:t}|$ considered in (6) by the factor $(1/(1 + VR_t/((1 - VR_t)(1/(1/k_s + 1/k_{sc}^{\mathrm{lv}})))))$ when the line supplies induction motor loads at LV. This factor is considerably lower than that for passive loads (e.g., 0.6 and 0.9 for induction motor loads and constant impedance loads, respectively, with $k_{sc}^{\mathrm{lv}} = 20$, $k_s = 6.7$, and $VR_t = 10\%$) implying that (6) given in IEC/TR 61000-3-13 is conservative for motor loads as expected. In other words, the impact of the term $Z_{++:t}I_{-:t/t}$ or the negative-sequence current $I_{-:t/t}$ on the resulting voltage $|V_-^{\mathrm{mv/t}}|$ cannot be ignored for induction motor loads as in the case of passive loads.

Fig. 3 illustrates the variation of $|V_-^{\mathrm{mv/t}}|$ with $|I_{+:t}|$ for the four load types established by using (10)–(13) in relation to the radial test system described in Appendix B ($|Z_{-+:t}| = 0.112\ \Omega$, $k_{sc}^{\mathrm{lv}} \approx 20$ and $k_s = 6.7$). It also gives the results obtained from unbalanced load-flow analysis (LF) justifying the new formulation.

5) Mix of Passive (P) and Induction Motor (IM) Loads: When the MV line supplies a mix of passive loads (at MV and/or LV) and induction motors (at LV), the negative-sequence current $I_{-:t/t}$ in (8) can be decomposed as

$$I_{-:t/t} = I_{-:p/t} + I_{-:\mathrm{im/t}} \tag{14}$$

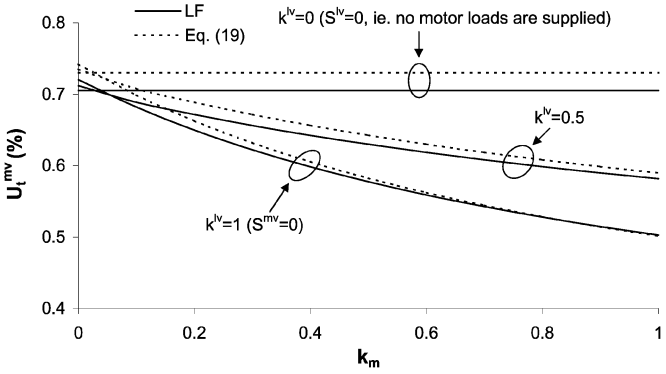

Fig. 4. Variation of U_t^{mv} with k_m for cases where $k^{\mathrm{lv}} = 1$, $k^{\mathrm{lv}} = 0.5$, and $k^{\mathrm{lv}} = 0$.

where $I_{-:p/t}$ and $I_{-:\mathrm{im/t}}$ are the negative-sequence currents (referred to MV) in passive (P) and induction motor (IM) branches, respectively, arising as a result of the asymmetrical MV line. Then, (8) can be expanded, employing (14) as

$$|V_-^{\mathrm{mv/t}}| = |Z_{-+:t}I_{+:t} + Z_{++:t}I_{-:p/t} + Z_{++:t}I_{-:\mathrm{im/t}}|. \tag{15}$$

The influence of the voltage component $Z_{++:t}I_{-:p/t}$ or the negative-sequence current $I_{-:p/t}$ corresponding to passive loads on the resulting $|V_-^{\mathrm{mv/t}}|$ can be reasonably ignored (as noted earlier). Thus, (15) can be simplified as

$$|V_-^{\mathrm{mv/t}}| \approx |Z_{-+:t}I_{+:t} + Z_{++:t}I_{-:\mathrm{im/t}}|. \tag{16}$$

Equation (16) can be written in a form similar to that of (9) as

$$|V_-^{\mathrm{mv/t}}| \approx |Z_{-+:t}I_{+:t}| \left| \frac{Z_{--}^{\mathrm{mv-im}}}{Z_{--}^{\mathrm{mv'-im}}} \right| \tag{17}$$

where $Z_{--}^{\mathrm{mv-im}}$, $Z_{--}^{\mathrm{mv'-im}}$ are the downstream negative-sequence impedances seen at the busbars MV and MV′, respectively, taking into account only induction motors supplied at LV. Expressing (17) in terms of line, system, and load characteristics, system operating conditions, and downstream load composition (Appendix C)

$$|V_-^{\mathrm{mv/t}}| \approx |Z_{-+:t}I_{+:t}| \frac{1}{1 + \left(\frac{VR_t}{1-VR_t}\right)\left(\frac{k^{\mathrm{lv}}}{\frac{1}{k_s k_m} + \frac{1}{k_{sc}^{\mathrm{lv}}}}\right)} \tag{18}$$

where k_m is the ratio between the rated motor load (in megavolt amperes) and the total load ($= S^{\mathrm{lv}}$) supplied by the LV busbar and $k^{\mathrm{lv}} = S^{\mathrm{lv}}/(S^{\mathrm{mv}} + S^{\mathrm{lv}})$ is the fraction of LV loads supplied by the busbar MV.

Voltage unbalance U_t^{mv} can be expressed in a generalized form by substituting (18) in (7) as

$$U_t^{\mathrm{mv}} \approx \frac{|Z_{-+:t}I_{+:t}|}{1 + \left(\frac{VR_t}{1-VR_t}\right)\left(\frac{k^{\mathrm{lv}}}{\frac{1}{k_s k_m} + \frac{1}{k_{sc}^{\mathrm{lv}}}}\right)} \times \frac{1}{|V_+^{\mathrm{mv}}|}. \tag{19}$$

Fig. 4 illustrates the variation of U_t^{mv} with k_m, established by using (19) in comparison to the results obtained from unbalanced load-flow analysis (LF) for the considered test system

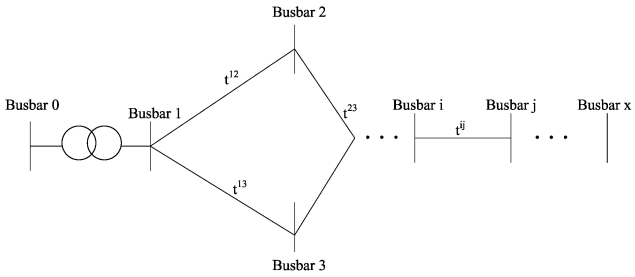

Fig. 5. Interconnected system.

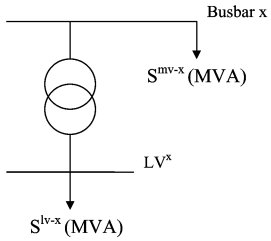

Fig. 6. Aggregated downstream system supplied by any busbar x of the interconnected system.

(Appendix B: $|Z_{-+:t}| = 0.112\ \Omega$, $k_{sc}^{\mathrm{lv}} \approx 20$, $k_s = 6.7$) in relation to three cases where:

- $k^{\mathrm{lv}} = 1$ (i.e., $S^{\mathrm{mv}} = 0$);
- $k^{\mathrm{lv}} = 0.5$;
- $k^{\mathrm{lv}} = 0$ (i.e., $S^{\mathrm{lv}} = 0$ and $k_m = 0$).

The operating scenario considered corresponds to $|I_{+:t}| \approx 470$ A, $VR_t \approx 8.5\%$, and $|V_+^{\mathrm{mv}}| \approx 7.2$ kV (1 p.u.). These results confirm the aforementioned basis describing the behavior of different load bases in relation to the global emission arising from line asymmetries while demonstrating the dependency of this emission on the motor proportion.

III. Methodology for Evaluating the Global Emission From Line Asymmetries

Consider the interconnected MV system shown in Fig. 5 where the MV lines $(t^{12}, t^{13}, t^{23}, \ldots, t^{ij})$ of interest are untransposed. The downstream system supplied by any busbar x is as per Fig. 6. For the purpose of assessing the emission arising from line asymmetries, the voltages at busbar 0, which represent the upstream high-voltage (HV) system and all loads supplied by the system, are taken as balanced.

The resulting negative-sequence voltage (V_-^x) at any busbar x which arises as a result of the interaction of the untransposed lines $t^{12}, t^{13}, t^{23}, \ldots, t^{ij}$ can be written as [7]

$$V_-^x = V_-^{x/t^{12}} + V_-^{x/t^{13}} + V_-^{x/t^{23}} + \cdots + V_-^{x/t^{ij}} \tag{20}$$

where $V_-^{x/t^{ij}}$ is the negative-sequence voltage caused by any line t^{ij} on its own at the busbar x. Then, the emission caused by the untransposed lines (U_{lines}^x) and the factor $K'ue(K'ue^x)$ at the busbar x can be expressed as given by (21) and (4), respectively

$$U_{\mathrm{lines}}^x = \left| \frac{V_-^x}{V_+^x} \right| \tag{21}$$

where V_+^x is the positive-sequence voltage at the busbar x.

Extending the nodal equations $[I] = [Y][V]$ (where $[I]$, $[Y]$, and $[V]$ are the nodal current, nodal admittance, and nodal voltage matrices, respectively) to the sequence domain xth element of $[I]$ (I^x), (x, y)th element of $[Y]$ (Y^{xy}), and xth element of $[V]$ (V^x) can be written, respectively, as

$$I^x = \begin{bmatrix} I_0^x \\ I_+^x \\ I_-^x \end{bmatrix} \tag{22}$$

$$Y^{xy} = \begin{bmatrix} Y_{00}^{xy} & Y_{0+}^{xy} & Y_{0-}^{xy} \\ Y_{+0}^{xy} & Y_{++}^{xy} & Y_{+-}^{xy} \\ Y_{-0}^{xy} & Y_{-+}^{xy} & Y_{--}^{xy} \end{bmatrix} \tag{23}$$

$$V^x = \begin{bmatrix} V_0^x \\ V_+^x \\ V_-^x \end{bmatrix} \tag{24}$$

where subscripts 0, $+$, and $-$ refer to the zero, positive, and negative sequences, respectively. Assuming negligible zero-sequence voltages and currents (i.e., $V_0^x = I_0^x = 0$), the nodal equations $[I] = [Y][V]$ of which the elements are given by (22)–(24) can be expanded to establish negative-sequence nodal currents $([I_-])$ as given by (25). Employing the relationship $Y_{--}^{xy} = Y_{++}^{xy}$ (for $x = y$ and $x \neq y$), (25) can be rewritten in a concise form as

$$\begin{bmatrix} -I_-^1 \\ -I_-^2 \\ \vdots \\ -I_-^n \end{bmatrix} = \begin{bmatrix} Y_{-+}^{11} & Y_{-+}^{12} & \cdots & Y_{-+}^{1n} \\ Y_{-+}^{21} & Y_{-+}^{22} & \cdots & Y_{-+}^{2n} \\ \vdots & \vdots & \vdots & \vdots \\ Y_{-+}^{n1} & Y_{-+}^{n2} & \cdots & Y_{-+}^{nn} \end{bmatrix} \begin{bmatrix} V_+^1 \\ V_+^2 \\ \vdots \\ V_+^n \end{bmatrix} + \begin{bmatrix} Y_{--}^{11} & Y_{--}^{12} & \cdots & Y_{--}^{1n} \\ Y_{--}^{21} & Y_{--}^{22} & \cdots & Y_{--}^{2n} \\ \vdots & \vdots & \vdots & \vdots \\ Y_{--}^{n1} & Y_{--}^{n2} & \cdots & Y_{--}^{nn} \end{bmatrix} \begin{bmatrix} V_-^1 \\ V_-^2 \\ \vdots \\ V_-^n \end{bmatrix} \tag{25}$$

$$-[I_-] = [Y_{-+}][V_+] + [Y_{++}][V_-]. \tag{26}$$

It was shown in Section II that the negative-sequence currents caused by line asymmetries make a significant impact on the global emission in the presence of large proportions of induction motor loads, although this impact can be reasonably ignored when the system supplies primarily passive loads. Thus, considering a mix of passive (supplied at MV and/or LV) and motor (supplied at LV) loads, the negative-sequence nodal current I_-^x at any busbar x can be written as

$$I_-^x \approx Y_{--}^{x-\mathrm{im}}\, V_-^x \tag{27}$$

where $Y_{--}^{x-\mathrm{im}}$ is the downstream negative-sequence admittance seen at the busbar x, taking into account only induction motors supplied at LV. This admittance $Y_{--}^{x-\mathrm{im}}$, which is inherently inductive due to the inductive nature of the associated induction motor negative-sequence impedances and MV–LV transformer impedances, can be expressed in terms of system and load characteristics, system operating conditions, and downstream load composition as

$$Y_{--}^{x-\mathrm{im}} \approx -j \left(\frac{k^{\mathrm{lv-x}}}{\frac{1}{k_{sc}^{\mathrm{lv-x}}} + \frac{1}{k_s^x k_m^x}} \right) \left(\frac{\sqrt{3}\, I_+^x}{V_n^{\mathrm{mv}}} \right) \tag{28}$$

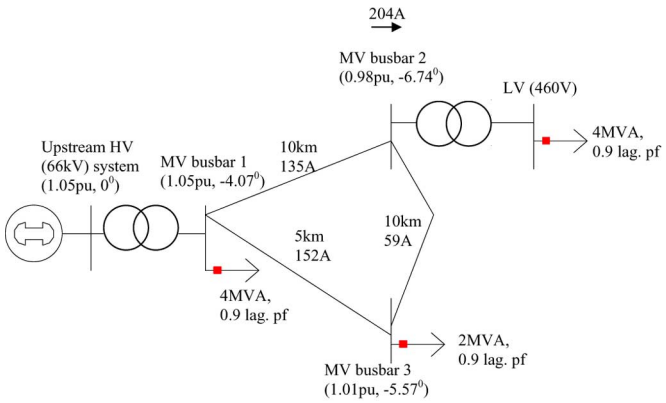

Fig. 7. Three-bus MV test system.

where $k^{\mathrm{lv-x}}$, $k_{sc}^{\mathrm{lv-x}}$, k_s^x, k_m^x as defined for (13) and (18) (additional superscripted x indicates the factors corresponding to the busbar x), and V_n^{mv} is the nominal line-to-line voltage of the MV system.

Substitution of (28) in (26) and the rearrangement gives

$$|[V_-]_{n\times 1}| \approx \left|[Y'^{-1}_{++}]_{n\times n}[Y_{-+}]_{n\times n}[V_+]_{n\times 1}\right| \qquad (29)$$

where

$$Y'^{xy}_{++} \approx Y^{xy}_{++} + Y^{x-\mathrm{im}}_{--} \text{ for } x = y$$
$$Y'^{xy}_{++} = Y^{xy}_{++} \text{ for } x \neq y.$$

That is, taking the nodal positive-sequence voltages as known quantities since they can be easily obtained from conventional balanced load-flow analysis, the nodal negative-sequence voltages arising due to line asymmetries can be established by using (29).

IV. Verification of the Methodology

The proposed methodology is applied to the simple three-bus MV system (60 Hz, 12.47 kV) shown in Fig. 7. Considering the operating scenario and resulting positive-sequence system conditions (which are established by using load-flow analysis) are also indicated in Fig. 7. Lengths of the lines which are taken as identical in construction (including phase positioning) and untransposed are shown alongside the lines. Relevant admittance data of the lines are (see Appendix B for further details): positive-sequence admittance $= (1.0098 - j2.0630)$ Skm, negative- and positive-sequence coupling admittance $= (0.0258 + j0.1821)$ Skm. Busbars 1 and 3 supply MV loads with equally shared constant impedance and constant power elements. That is, $k_m^x = 0$ implying $Y^{x-\mathrm{im}}_{--} \approx 0$ for $x = 1, 3$. Busbar 2 (i.e., $x = 2$) supplies loads at LV which account for 40% of the total load supplied by the system. Two cases based on the type of LV loads are considered as follows.

Case 1) LV loads represent passive loads (equally shared constant power and constant impedance elements) or $k_m^x = 0$. That is, $Y^{x-\mathrm{im}}_{--} \approx 0$.

Case 2) LV loads represent three-phase induction motors or $k_m^x = 1$. The aggregation of 50-hp motors of which the details are given in Appendix B is considered. This results in an admittance $Y^{x-\mathrm{im}}_{--} \approx -j0.1316$ S.

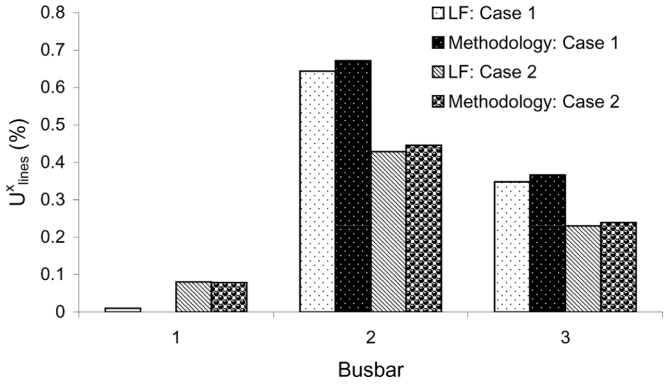

Fig. 8. Emission U^x_{lines} for the three-bus MV test system.

Fig. 8 illustrates the emission U^x_{lines} at the MV busbars for the two cases mentioned before. This shows the results established by using the methodology in comparison to the results obtained from unbalanced load-flow analysis (LF), demonstrating the accuracy of the proposed technique. Further, these results reveal that the presence of considerable proportions of induction motor loads increases the emission U^x_{lines} at the busbar which is directly connected to the upstream system (e.g., busbar 1 in Fig. 7) relative to that corresponding to passive loads. In addition, induction motor loads help reduce the emission U^x_{lines} at all other busbars (e.g., busbars 2 and 3 in Fig. 7) relative to that corresponding to passive loads.

V. Conclusion

The paper has addressed the global voltage unbalance in MV power systems arising as a result of line asymmetries which is an important aspect in assessing voltage unbalance emission limits to unbalanced installations connected to MV power systems based on the IEC/TR 61000-3-13 guidelines. The dependency of this global emission on various load types, including three-phase induction motor loads, has been examined by using a simple radial network. Major conclusions can be drawn from the study as follows.

- Direction given in IEC/TR 61000-3-13 to assess the influence of an asymmetrical and radial line on the global emission can be applied to an MV network only when the system supplies primarily passive loads. In this case, the impact of the negative-sequence currents arising as a result of line asymmetries on the global emission is insignificant.
- However, the direction given in IEC/TR 61000-3-13 has been seen to be conservative when the network supplies a large proportion of induction motor loads. In this case, the negative-sequence currents arising as a result of line asymmetries make a significant influence on the global emission.

A systematic approach, covering radial and interconnected networks, for evaluating the global emission caused by line asymmetries at the nodal-level taking line, system, and load characteristics, system operating conditions, and downstream load composition into account have been proposed. The results

established by using the proposed methodology in relation to a three-bus test system have been seen to be in close agreement with the results obtained from unbalanced load-flow analysis. Further, these results clearly demonstrated the following:

- presence of considerable proportions of induction motor loads at downstream LV systems increases the global emission at the MV busbar which is directly connected to the upstream system relative to that corresponding to passive loads;
- induction motor loads help to reduce the global emission levels at all other busbars of the network relative to that corresponding to passive loads.

APPENDIX A

When S^{mv} and S^{lv} of the system shown in Fig. 2 represent constant impedance loads, the currents $I_{+:t}$ and $I_{-:t/t}$ in (8) can be written,[6] respectively, as

$$I_{+:t} = \frac{V_{+}^{\mathrm{mv}}}{Z_{++}^{\mathrm{mv}'}} \tag{A1}$$

$$I_{-:t/t} = Y_{-+}^{\mathrm{mv}'}\, V_{+}^{\mathrm{mv}'}. \tag{A2}$$

Downstream negative- and positive-sequence coupling admittance seen at a busbar x (Y_{-+}^{x}) of a radial network can be expressed by using various impedance elements seen at the busbar[7] as

$$Y_{-+}^{x} \approx \frac{-Z_{-+}^{x}}{Z_{++}^{x}\, Z_{--}^{x}}. \tag{A3}$$

Alternatively, the downstream negative- and positive-sequence coupling impedance seen at the busbar x (Z_{-+}^{x}) can be expressed by using various admittance elements seen at the busbar x as

$$Z_{-+:x} \approx \frac{-Y_{-+}^{x}}{Y_{++}^{x}\, Y_{--}^{x}} \tag{A4}$$

where Z_{++}^{x}, Z_{--}^{x} is the downstream positive and negative sequence impedances respectively seen at the busbar x, and Y_{++}^{x}, Y_{--}^{x} is the downstream positive- and negative-sequence admittances, respectively, seen at the busbar x

For the considered system where the loads are balanced (i.e., decoupled sequence impedances) and the MV line is untransposed: $Z_{-+}^{\mathrm{mv}'} = Z_{-+:t}$. Thus, the admittance $Y_{-+}^{\mathrm{mv}'}$ can be given by

$$Y_{-+}^{\mathrm{mv}'} \approx \frac{-Z_{-+:t}}{Z_{++}^{\mathrm{mv}'}\, Z_{--}^{\mathrm{mv}'}}. \tag{A5}$$

Substituting (A.1), (A.2), and (A.5) in (8)

$$|V_{-}^{\mathrm{mv/t}}| = |Z_{-+:t} I_{+:t}| \left| \frac{Z_{--}^{\mathrm{mv}}}{Z_{--}^{\mathrm{mv}'}} \right| \tag{A6}$$

[6]Note that the voltages at the sending-end busbar of the line are balanced.

[7]Through the inversion of the impedance matrix and the simplification by ignoring some of the terms.

APPENDIX B

The MV line [10]—12.47-kV, three-wired, 3.2187-km, 1.143-m horizontal build, untransposed, phase positioning: ◯a ◯ b ◯ c, conductor geometric mean radius = 7.7724 mm, conductor resistance = 0.19014 Ω/km, earth resistivity = 100 Ωm, $Z_{++} = 0.1901 + j0.3937$ Ω/km, $Z_{-+} = 0.0302 + j0.0174$ Ω/km.

The MV–LV transformer [10]—aggregation of fully loaded 1-MVA, 12.47-kV/460-V, 60-Hz transformers with $X = 5\%$ and $R = 1\%$ and secondary tap setting = 1.03 p.u. This gives $k_{sc}^{\mathrm{lv}} \approx 20$.

The induction motor load (supplied at LV)—aggregation of 50-hp, 460-V, 1705 r/min three-phase induction motors [11] supply the rated mechanical load. The parameters per motor are $r_s = 0.087$ Ω, $r_r' = 0.228$ Ω, $x_s = x_r' = 0.302$ Ω, $x_m = 13.08$ Ω (under the rated operating conditions, input power = 50 kVA at 0.9 lag. pf and $k_s = 6.7$).

Passive loads (supplied at LV and/or MV)—aggregation of passive components with rated power of 50 kVA at 0.9 lag. pf, which consists of equally shared constant power and constant impedance elements.

The operating scenario considered in Fig. 4—$V_{+}^{\mathrm{mv}'} = 1.08\angle 0^{0}$ p.u., total load supplied by the MV line = 10 MVA at 0.9 lag. pf. Resulting system conditions are as follows: $I_{+:t} \approx 470A$ $VR_t \approx 8.5\%$, $|V_{+}^{\mathrm{mv}}| \approx 7.2$ kV (1 p.u.).

APPENDIX C

Noting that $Z_{--}^{\mathrm{mv}'-\mathrm{im}} = Z_{--}^{\mathrm{mv}-\mathrm{im}} + Z_{++:t}$ and the inductive nature of the associated impedance elements (e.g., $Z_{--}^{\mathrm{mv}-\mathrm{im}}$ is made up of negative-sequence impedances of induction motors and MV–LV transformers), (17) can be rearranged as

$$\left| \frac{Z_{++}^{\mathrm{mv}}}{Z_{--}^{\mathrm{mv}-\mathrm{im}}} \right| \approx \frac{1}{(S^{\mathrm{mv}} + S^{\mathrm{lv}})} \times \left(\frac{1}{\left| \frac{Z_{--:im}}{Z_{++:im}} \right| \left| \frac{Z_{++:\mathrm{im}}}{Z_{++}^{\mathrm{lv}}} \right| \frac{|Z_{++}^{\mathrm{lv}}|}{|V_{+}^{\mathrm{lv}}|^2} + \frac{|Z_{++:\mathrm{ml-lv}}|}{|V_{+}^{\mathrm{lv}}|^2}} \right). \tag{C1}$$

$$|V_{-}^{\mathrm{mv/t}}| \approx |Z_{-+:t} I_{+:t}| \left(\frac{1}{1 + \left| \frac{Z_{++:t}}{Z_{++}^{\mathrm{mv}}} \right| \left| \frac{Z_{++}^{\mathrm{mv}}}{Z_{--}^{\mathrm{mv-im}}} \right|} \right). \tag{C2}$$

The ratio $\left| Z_{++:t} / Z_{++}^{\mathrm{mv}} \right|$ can be expressed as

$$\left| \frac{Z_{++:t}}{Z_{++}^{\mathrm{mv}}} \right| \approx \frac{VR_t}{1 - VR_t}. \tag{C3}$$

Substituting $Z_{--}^{\mathrm{mv}-\mathrm{im}} = (n_{\mathrm{ml}})^2 (Z_{--:im} + Z_{++:\mathrm{ml-lv}})$ and rearranging, the ratio $\left| Z_{++}^{\mathrm{mv}} / Z_{--}^{\mathrm{mv}-\mathrm{im}} \right|$ can be written as

$$\left| \frac{Z_{++}^{\mathrm{mv}}}{Z_{--}^{\mathrm{mv}-\mathrm{im}}} \right| = \left(\frac{1}{\frac{(n_{\mathrm{ml}})^2 |Z_{--:\mathrm{im}} + Z_{++:\mathrm{ml-lv}}|}{|V_{+}^{\mathrm{mv}}|^2}} \right) \left(\frac{1}{\frac{|V_{+}^{\mathrm{mv}}|^2}{|Z_{++}^{\mathrm{mv}}|}} \right) \tag{C4}$$

where $n_{\rm ml}$ is the operating turns ratio of the MV–LV transformer and $Z_{--:im}$ is the negative-sequence impedance of the motor load.

The term $|V_+^{\rm mv}|^2/|Z_{++}^{\rm mv}|$ represents the total megavolt-ampere load load $(S^{\rm mv} + S^{\rm lv})$ supplied by the busbar MV. Employing $|V_+^{\rm mv}| = n_{\rm ml}|V_+^{\rm lv}|$ and $|Z_{--:\rm im} + Z_{++:\rm ml-lv}| \approx |Z_{--:\rm im}| + |Z_{++:\rm ml-lv}|$ (where $Z_{++:\rm im}$ is the positive-sequence impedance of the motor load), (C4) can be further rearranged as given by (C1). Noting that

$$\left|\frac{Z_{--:\rm im}}{Z_{++:\rm im}}\right| = \frac{1}{k_s}, \quad \left|\frac{Z_{++:\rm im}}{Z_{++}^{\rm lv}}\right| = \frac{1}{k_{\rm m}}, \quad \frac{|Z_{++}^{\rm lv}|}{|V_+^{\rm lv}|^2} = \frac{1}{S^{\rm lv}}$$
$$\frac{|Z_{++:\rm ml-lv}|}{|V_+^{\rm lv}|^2} = \frac{1}{\rm SSC^{lv}}, \quad \frac{S^{\rm lv}}{S^{\rm mv}+S^{\rm lv}} = k^{\rm lv},$$
$$\frac{\rm SSC^{lv}}{S^{\rm lv}} = k_{sc}^{\rm lv}$$

Equation (C1) can be expressed as

$$\left|\frac{Z_{++}^{\rm mv}}{Z_{--}^{\rm mv-im}}\right| \approx \frac{k^{\rm lv}}{\frac{1}{k_s k_m} + \frac{1}{k_{sc}^{\rm lv}}}. \tag{C5}$$

The substitution of (C3) and (C5) in (C2) gives

$$|V_-^{\rm mv/t}| \approx |Z_{-+:t} I_{+:t}| \frac{1}{1 + \left(\frac{VR_t}{1-VR_t}\right)\left(\frac{k^{\rm lv}}{\frac{1}{k_s k_m}+\frac{1}{k_{sc}^{\rm lv}}}\right)}. \tag{C6}$$

REFERENCES

[1] "Assesment of emission limits for the connection of disturbing installtions to power systems," Joint Working Group CIGRE/CIRED C4.103 (formely CIGRE C4.06), 2007, Final Rep.

[2] R. Koch, G. Beaulieu, L. Berthet, and M. Halpin, "International survey of unbalance levels in LV, MV, HV and EHV power systems: CIGRE/CIRED JWG C4.103 results," in *Proc. 19th Int. Conf. Electricity Distribution*, Vienna, Austria, May 2007, pp. 21–24, paper 0892.

[3] R. Koch, G. Beaulieu, L. Berthet, and M. Halpin, "Recommended methods of determining power qality emission limits for installations connected to EHV, HV, MV and LV power systems," in *Proc. 19th Int. Conf. Electricity Distribution*, Vienna, Austria, May 2007, pp. 21–24, paper 0893.

[4] "Electromagnetic compatibility (EMC)—limits—Assessment of emission limits for the connection of unbalanced installations to MV, HV and EHV power systems," IEC Tech. Rep. 61000-3-13, 2008.

[5] "Electromagnetic compatibility (EMC)—limits—assessment of emission limits for distorting loads in MV and HV power systems," IEC Tech. Rep. 61000-3-6, 1996.

[6] "Electromagnetic compatibility (EMC)—limits—assessment of emission limits for fluctuating loads in mv and hv power systems," IEC Tech. Rep. 61000-3-7, 1996.

[7] P. Paranavithana, S. Perera, and D. Sutanto, "Analysis of system asymmetry of interconnected 66 kV sub-transmission systems in relation to voltage unbalance," in *Proc. IEEE Power Eng. Soc. PowerAfrica 2007 Conf. Expo.*, Johannesburg, South Africa, Jul. 2007, pp. 16–20, paper 35.

[8] P. Paranavithana, S. Perera, and R. Koch, "An improved methodology for determining MV to LV voltage unbalance transfer coefficient," presented at the 13th Int. Conf. Harmonics Quality Power, Wollongong, Australia, Sep. 28–Oct. 1, 2008.

[9] P. Paranavithana, S. Perera, and D. Sutanto, "Impact of untransposed 66 kV sub-transmission lines on voltage unbalance," presented at the Australasian Universities Power Engineering Conf., Melbourne, Australia, Dec. 2006, paper 28.

[10] R. C. Dugan, "Induction machine modeling for distribution system analysis—Test case description," in *Proc. Power Eng. Soc. Transm. Distrib.*, May 21–24, 2006, pp. 578–582.

[11] P. C. Krause, O. Wasynczuk, and S. D. Sudhoff, *Analysis of Electric Machinery and Drive Systems*, 2nd ed. New York: Wiley, 2002, pp. 165–165.

[12] J. D. Glover and G. Digby, *Preliminary Edition, Software Manual—Power System Analdysis and Design*, 2nd ed. Boston, MA: PWS, 1994, pp. 87–87.

P. Paranavithana (S'07) received the B.Sc.(Eng) (Hons.) degree in electrical power engineering from the University of Moratuwa, Moratuwa, Sri Lanka, in 2005 and is currently pursuing the Ph.D. degree in electrical power engineering at the University of Wollongong, Wollongong, Australia.

Her research interests are in power quality and power system analysis.

S. Perera (M'95) received the B.Sc. (Eng) degree in electrical power engineering from the University of Moratuwa, Moratuwa, Sri Lanka, the M.Eng.Sc. degree in electrical engineering from the University of New South Wales, Sydney, Australia, and the Ph.D. degree in electrical engineering from the University of Wollongong, Wollongong, Australia.

He has been a Lecturer at the University of Moratuwa. Currently he is an Associate Professor with the University of Wollongong. He is the Technical Director of the Integral Energy Power Quality and Reliability Centre at the University of Wollongong.

R. Koch received the B.Eng. and M.Eng. degrees in electrical power engineering from the University of Stellenbosch, Stellenbosch, South Africa.

He is a Corporate Specialist with Eskom Holdings Ltd., South Africa, and Convener of IEC 77A/WG8—the working group responsible for publishing IEC/TR 61000-3-13.

Mr. Koch is an active participant in CIGRE working groups—and was the document coordinator for the CIGRE report on which IEC 61000-3-13 was based. Currently, he is the Convener of Advisory Group C4.1 (Power Quality), of the Study Committee C4 (System Technical Performance).

Z. Emin received the B.Sc. degree in electrical and electronics engineering from Middle East Technical University, Ankara, Turkey, and the M.Sc. and Ph.D. degrees from The University of Manchester, Manchester, U.K.

He leads a team of specialist power system engineers who are responsible for undertaking detailed analysis of the quality of supply aspects of system performance for new connections, infrastructure, and asset-replacement schemes to ensure Grid Code compliance.

Dr. Emin is a registered Chartered Engineer in the U.K. and a member of the Institute of Engineering and Technology. He is the U.K. representative on CIGRE Study Committee C4 System Technical Performance. He was a corresponding member with the CIGRE/CIRED Joint Working Group C4.103.